Diffusion constants from the recursion method

Jiaozi Wang ⬤, Mats H. Lamann, Robin Steinigeweg ⬤, and Jochen Gemmer
Department of Mathematics/Computer Science/Physics, University of Osnabrück, Osnabrück D-49076, Germany

Understanding the transport behavior of quantum many-body systems constitutes an important physical endeavor, both experimentally and theoretically. While a reliable classification into normal and anomalous dynamics is known to be notoriously difficult for a given microscopic model, even the seemingly simpler evaluation of transport coefficients in diffusive systems continues to be a hard task in practice. This fact has motivated the development and application of various sophisticated methods and is also the main issue of this paper. We particularly take a barely used strategy, which is based on the recursion method, and demonstrate that this strategy allows for accurate calculation of diffusion constants for different paradigmatic examples, including magnetization transport in nonintegrable spin-1/2 chains and ladders as well as energy transport in the mixed-field Ising model in one dimension.

I. INTRODUCTION

Dynamics in quantum many-body systems constitutes a central question in various disciplines of modern physics [1–7]. In particular, transport is a paradigmatic example of a dynamical process and is concerned with the flow of a globally conserved quantity through a given system in the course of time. While the study of transport has a long and fertile history, it continues to be in the focus of ongoing research [7], both experimentally and theoretically. A particular challenge is understanding the behavior in the hydrodynamic regime, i.e., at large length scales and in the long-time limit.

Within the class of physically relevant models, integrable systems play a special role [8]. While the flow of energy is typically ballistic in such systems, a richer phase diagram can result for other transport quantities. A prime example in this context is the prominent spin-1/2 XXZ model, which features ballistic, superdiffusive, and diffusive dynamics in different parameter regions [7]. On the one hand, the origin of ballistic dynamics has been traced back to (quasi)local conserved quantities [9–11]. On the other hand, other nonballistic types of dynamics have been identified by the combination of complementary analytical and numerical techniques over many years. Recent progress is based on generalized hydrodynamics [12,13], which yields a comprehensive framework in all parameter regimes. Similarly, rich features can be also found in quantum many-body models with disorder [14,15], long-range interactions [16,17], or constraints [18,19].

Integrable systems are the exception rather than the rule, and nonintegrable systems represent the generic case. These systems add another level of complexity, as they do not allow for an exact analytical treatment in the thermodynamic limit. Still, a natural assumption for these models is the emergence of diffusive dynamics [7], e.g., due to the onset of chaos and thermalization. However, this assumption has as such no consequence for the value of the actual transport coefficient. And in fact, the intricate calculation of transport in nonintegrable and integrable systems has been

one motivation for the development and application of sophisticated approaches, where each approach has its own advantage and disadvantage. These approaches range from perturbation theory [20–22], over exact and Lanczos diagonalization [23–25], quantum typicality [26,27], time-dependent density-matrix renormalization group for correlation functions or wave packets [28–30], quantum Monte-Carlo [31,32], Lindblad formulation of steady-state transport [33–35], to semiclassical and classical treatment [36–38], and probably many more.

In view of this situation, this paper takes a fresh perspective and barely explored strategy, which is based on the recursion method [39–45]. In one of the few works that pursue a similar approach, the authors employ a so-called modified Mori theory to arrive at transport coefficients [40]. (Results similar to those in Ref. [40] have also been reported later in Ref. [46].) This approach requires the knowledge of sufficiently many "Lanczos coefficients" (for definition see below). However, it was never applied to transport in specific interacting quantum models, most likely since the computation of the Lanczos coefficients practically requires modern computing power. Another way to compute diffusion constants from a finite set of Lanczos coefficients has recently been suggested and applied to energy transport in a tilted-field Ising chain in Ref. [41]. This approach is based on the *operator growth hypothesis*, similar to the technique suggested in the current paper. The main difference is that the latter employs the linear response theory, whereas the former does not. As a consequence, the present approach is substantially more efficient, especially in the thermodynamic limit. This opens for otherwise challenging analyses, for example, the insensitivity of the computed diffusion coefficient to the number of actually employed Lanczos coefficients, the absence of which may indicate ballistic behavior, becomes feasible, as will be detailed below.

We demonstrate that our strategy practically and consistently allows for the accurate calculation of diffusion constants for different paradigmatic examples, including

magnetization transport in nonintegrable spin-1/2 chains and ladders as well as energy transport in the mixed-field Ising model in one dimension, and compare to values from the literature [47–52].

II. MODELS AND CURRENTS

In this paper, we consider three different paradigmatic examples of quantum many-body systems, which have also attracted significant attention in the literature on transport before. The first model is a perturbed XXZ spin-1/2 chain [7],

$$H = \sum_{r=1}^{L} \left(s_r^x s_{r+1}^x + s_r^y s_{r+1}^y + \Delta s_r^z s_{r+1}^z + \Delta' s_r^z s_{r+2}^z \right), \quad (1)$$

where s_r^i $(i = x, y, z)$ are the components of a spin-1/2 operator at lattice site r, L is the total number of lattice sites, and Δ, Δ' are anisotropies in the z direction. For $\Delta' = 0$, the model is integrable in terms of the Bethe *Ansatz* while, for any $\Delta' \neq 0$, this integrability is broken. For all values of Δ, Δ', the total magnetization $S^z = \sum_r s_r^z$ is conserved, i.e., transport of local magnetizations s_r^z is a meaningful question. Note that, for this model and the other models below, periodic boundary conditions are employed.

The second model is a XX spin-1/2 ladder [47–49]. It is chosen as an example for a quasi-onedimensional system, and its Hamiltonian is given by $H = J_\parallel H_\parallel + J_\perp H_\perp$, where

$$H_\parallel = \sum_{i=1}^{L} \sum_{l=1}^{2} \left(s_{r,l}^x s_{r+1,l}^x + s_{r,l}^y s_{r+1,l}^y \right),$$

$$H_\perp = \sum_{r=1}^{L} \left(s_{r,1}^x s_{r,2}^x + s_{r,1}^y s_{r,2}^y \right) \quad (2)$$

are the Hamiltonians of the legs and rungs, respectively, with corresponding exchange coupling constants $J_\parallel$ and $J_\perp$. For $J_\perp = 0$, the model is integrable and identical to noninteracting fermions by means of the Jordan-Wigner transformation while, for any $J_\perp > 0$, the integrability is broken again. As before, for all values of $J_\parallel$, $J_\perp$, the total magnetization $S^z = \sum_{r,l} s_{r,l}^z$ is conserved.

The third and last model is the Ising spin-1/2 chain in the presence of a mixed field [49–51]. Its Hamiltonian can be written as $H = \sum_{r=1}^{L} h_r$,

$$h_r = 4 s_r^z s_{r+1}^z + B_x \left(s_r^x + s_{r+1}^x \right) + B_z \left(s_r^z + s_{r+1}^z \right), \quad (3)$$

where B_x and B_z are the strengths of the field in x and z direction, respectively. The integrability of the model for $B_x = 0$ or $B_z = 0$ is broken for other values of B_x, B_z. In contrast to the previous models, the total energy H is the only nontrivial conserved quantity, i.e., transport of local energies h_r is meaningful here.

A natural strategy for the investigation of transport is given by currents [7]. The definition of local currents follows from the continuity equation

$$\dot{q}_r = i[H, q_r] = j_{r-1} - j_r, \quad (4)$$

where q_r is the local transport quantity, i.e., either local magnetizations s_r, $s_{r,l}$ or local energies h_r for the models in this

paper. Within the theory of linear response, the autocorrelation function of the total current $J = \sum_r j_r$ plays a central role and reads

$$\langle J(t)J \rangle = \frac{\text{tr}[e^{-\beta H} e^{iHt} J e^{-iHt} J]}{Z}, \quad Z = \text{tr}[e^{-\beta H}], \quad (5)$$

where $\beta = 1/T$ is the inverse temperature, which we set to the still nontrivial value $\beta = 0$ in the following. To determine transport coefficients, one can then define the quantity [53]

$$D(t) = \frac{1}{\chi} \int_0^t dt' \langle J(t')J \rangle, \quad \chi = \langle Q^2 \rangle - \langle Q \rangle^2, \quad (6)$$

where $Q = \sum_r q_r$ and χ is the static susceptibility. (For the three models in this paper, expressions for χ and J can be found in the Appendixes). For a diffusive system, the diffusion constant is given by $D = \lim_{t \to \infty} D(t)$, provided that the thermodynamic limit is taken first. It is worth pointing out that the quantity $D(t)$ additionally contains information at finite time and length scales, as well as on other transport types [53]. As apparent from Eq. (6), it is crucial to determine the area under the autocorrelation function. While various approaches to this area have been applied in the literature before, we take in this paper a barely used strategy, which is based on the recursion method.

III. FRAMEWORK AND ANALYTICAL RESULTS

In the following, it is quite convenient to switch to the Hilbert of space of operators and denote its elements O by states $|O)$. This space is equipped with an inner product $(O_m|O_n) = \text{tr}[O_m^\dagger O_n]$, which defines a norm via $||O|| = \sqrt{(O|O)}/\text{tr}[\mathbb{1}]$. The Liouvillian superoperator is defined by $\mathcal{L}|O) = [H, O]$ and propagates a state $|O)$ in time, such that an autocorrelation function can be written as $\langle O(t)O \rangle \propto C(t) = (O|e^{i\mathcal{L}t}|O)/||O||^2$.

The Lanczos algorithm can be employed to obtain a tridiagonal representation of $\mathcal{L}$ in a subspace determined by some "seed" O. In this paper, we have $O = J$. To start the iterative scheme, we take a normalized initial state $|O_0) \propto |O)$, i.e., $(O_0|O_0) = 1$, and set $b_1 = \|\mathcal{L}O_0\|$ as well as $|O_1) = \mathcal{L}|O_0)/b_1$. Then, we iteratively compute

$$|O_n') = \mathcal{L}|O_{n-1}) - b_{n-1}|O_{n-2}),$$
$$b_n = ||O_n'||,$$
$$|O_n) = |O_n')/b_n. \quad (7)$$

The tridiagonal representation of $\mathcal{L}$ in the Krylov basis $\{|O_n)\}$ results as

$$\mathcal{L}_{mn} = (O_m|\mathcal{L}|O_n) = \begin{pmatrix} 0 & b_1 & 0 & \cdots \\ b_1 & 0 & b_2 & \\ 0 & b_2 & 0 & \ddots \\ \vdots & & \ddots & \ddots \end{pmatrix}_{mn}, \quad (8)$$

where the Lanczos coefficients b_n are real and positive numbers. Their iterative computation is an elementary part of the recursion method. For the remainder of this paper, we denote $|O_n)$ by $|n)$ for simplicity.

In the context of the Mori theory [40,54], the time evolution of a set of functions $C_n(t)$ can be expressed in terms of a set

of integro-differential equations (see Appendixes for details),

$$\dot{C}_n(t) = -b_{n+1}^2 \int_0^t \mathrm{d}t' \, C_{n+1}(t-t') C_n(t'), \tag{9}$$

$C_0(t) = C(t)$, and $C_n(t) = (n|e^{i\mathcal{L}_n t}|n)$. The operator $\mathcal{L}_n$ is a "submatrix" of $\mathcal{L}$ and defined as

$$\mathcal{L}_n = \sum_{m=n+1} b_m[|m+1)(m| + |m)(m+1|]. \tag{10}$$

Employing the Laplace transform of $C_n(t)$,

$$F_n(s) = \int_0^\infty \mathrm{d}t \, e^{-st} C_n(t), \tag{11}$$

one gets from Eq. (9) the expression

$$F_n(s) = \frac{1}{s + b_{n+1}^2 F_{n+1}(s)}. \tag{12}$$

Thus, the Laplace transform of $C_0(t)$ can be written in the form

$$F_0(s) = \frac{1}{s + \dfrac{b_1^2}{s + \dfrac{b_2^2}{s + \dfrac{b_3^2}{s + \dots}}}}. \tag{13}$$

Then, recalling the definition of the diffusion constant in Eq. (6), one has $D = \langle J^2 \rangle F_0(0)/\chi$ and, using Eq. (13) and iterating up to R, one has

$$F_0(0) = \begin{cases} F_R(0) \prod_{m=1}^{\frac{R}{2}} \frac{b_{2m}^2}{b_{2m-1}^2}, & \text{even } R \\ \frac{1}{b_R^2 F_R(0)} \prod_{m=1}^{\frac{R-1}{2}} \frac{b_{2m}^2}{b_{2m-1}^2}, & \text{odd } R \end{cases}. \tag{14}$$

To further simplify the expression, we write $F_R(0)$ as

$$F_R(0) = \frac{1}{b_{R+1}} \int_0^\infty (R|e^{i\frac{\mathcal{L}_R}{b_{R+1}}(b_{R+1}t)}|R) \, \mathrm{d}(b_{R+1}t) \tag{15}$$

and $F_R(0) = p_{R+1}/b_{R+1}$ with the dimensionless quantity

$$p_{R+1} = \int_0^\infty (R|e^{i\frac{\mathcal{L}_R}{b_{R+1}}t}|R) \, \mathrm{d}t = \prod_{m=1}^\infty \left(\frac{b_{R+m}}{b_{R+m+1}}\right)^{(-1)^m}. \tag{16}$$

Therefore Eq. (14) can be written as

$$F_0(0) = \begin{cases} \frac{1}{p_R b_R} \prod_{m=1}^{\frac{R}{2}} \frac{b_{2m}^2}{b_{2m-1}^2}, & \text{even } R \\ \frac{p_R}{b_R} \prod_{m=1}^{\frac{R-1}{2}} \frac{b_{2m}^2}{b_{2m-1}^2}, & \text{odd } R \end{cases}. \tag{17}$$

Up to this point, everything is rigorous. If all b_n are known, p_R can be calculated using Eq. (16) and $F_0(0)$ can be obtained to arbitrary precision. In practice, however, only several of the first b_n are easily accessible. So, the question is to find a good estimation of p_R from those b_n which are numerically accessible. To this end, we employ the *operator growth hypothesis* introduced in Ref. [41], which states that, in a chaotic system, the b_n have for sufficiently large n the asymptotic form

$$b_n = \begin{cases} A\frac{n}{\ln n} + o(\frac{n}{\ln n}), & d = 1 \\ \alpha n + \beta + o(1), & d > 1 \end{cases}. \tag{18}$$

For dimension $d > 1$, neglecting the $o(1)$ term, one can derive an analytical expression for p_R,

$$p_R = \frac{\Gamma\left(\frac{R}{2} + \frac{\beta}{2\alpha}\right)\Gamma\left(\frac{R}{2} + \frac{\beta}{2\alpha} + 1\right)}{\Gamma^2\left(\frac{R}{2} + \frac{\beta}{2\alpha} + \frac{1}{2}\right)}. \tag{19}$$

For $d = 1$, on top of the linear behavior, there is also a logarithmic correction. If this correction only enters at very large n, one can show that Eq. (19) still holds approximately.

Here, we use a rather simple approach, where α and β are determined by b_R and b_{R-1} only, i.e., $\alpha_R = b_R - b_{R-1}$ and $\beta_R = Rb_{R-1} - (R-1)b_R$. This approach yields

$$p_R \simeq \tilde{p}_R = \frac{\Gamma\left(\frac{R}{2} + \frac{\beta_R}{2\alpha_R}\right)\Gamma\left(\frac{R}{2} + \frac{\beta_R}{2\alpha_R} + 1\right)}{\Gamma^2\left(\frac{R}{2} + \frac{\beta_R}{2\alpha_R} + \frac{1}{2}\right)}. \tag{20}$$

Then, substituting Eqs. (20) to (17), one obtains an approximation of $F_0(0)$,

$$F_0^{(R)}(0) = \begin{cases} \frac{1}{\tilde{p}_R b_R} \prod_{m=1}^{\frac{R}{2}} \frac{b_{2m}^2}{b_{2m-1}^2}, & \text{even } R \\ \frac{\tilde{p}_R}{b_R} \prod_{m=1}^{\frac{R-1}{2}} \frac{b_{2m}^2}{b_{2m-1}^2}, & \text{odd } R \end{cases}. \tag{21}$$

It can be shown (in Appendixes) that $\tilde{p}_R \to 1$ for $R \to \infty$ (or $\frac{\beta_R}{\alpha_R} \to \infty$). In this large R case Eq. (21) is almost identical to a result in Ref. [40], which is based on an ad hoc assumption and has never been applied to specific many body systems, as already outlined in the introduction. Correspondingly, one obtains an approximation of the diffusion constant,

$$D \simeq D_R = \frac{\langle J^2 \rangle}{\chi} F_0^{(R)}(0), \tag{22}$$

which is a main result of this paper.

IV. NUMERICAL RESULTS

Now, we check the estimation of D in Eq. (22) for the three different examples of quantum many-body systems, with a focus on model parameters in the nonintegrable regime. First, we numerically calculate the Lanczos coefficients b_n in Figs. 1(a), 2(a), and 3(a), respectively. As visible in these figures, a region with an approximately linear scaling of b_n is observed in all cases considered.

Next, we depict the corresponding estimates of D in Figs. 1(b), 2(b), and 3(b). Remarkably, we observe in Figs. 1(b) and 2(b) that D_R saturates at a constant value for $R \approx 5$ already, while in Fig. 3(b) the saturation is less clear. To check whether the value of D_R indeed provides a good estimate of the true D, we compare the results to existing numerical results in the literature [47–52], where values for D have been determined for the same model parameters. An almost perfect agreement with the estimate is found in the XXZ model ($\Delta = 0.5$) and XX ladder shown in Figs. 1(b) and 2(b). In the Ising model ($B_x = 1.05$, $B_z = 0.5$), $D_R(R \approx 40)$ approximately agrees with the results in Ref. [41] with a deviation by a few percent [55]. Slightly larger deviation ($\approx 10\%$) is observed at $B_x = 1.4$, $B_z = 0.9045$ [Fig. 3(b)]. Whether or not this deviation would vanish if more b_n (beyond $n=44$) were taken into account remains unclear within our investigation, due to numerical limitations. However, up to $R \approx 40$ the D_R do not exhibit a systematic trend, rather they
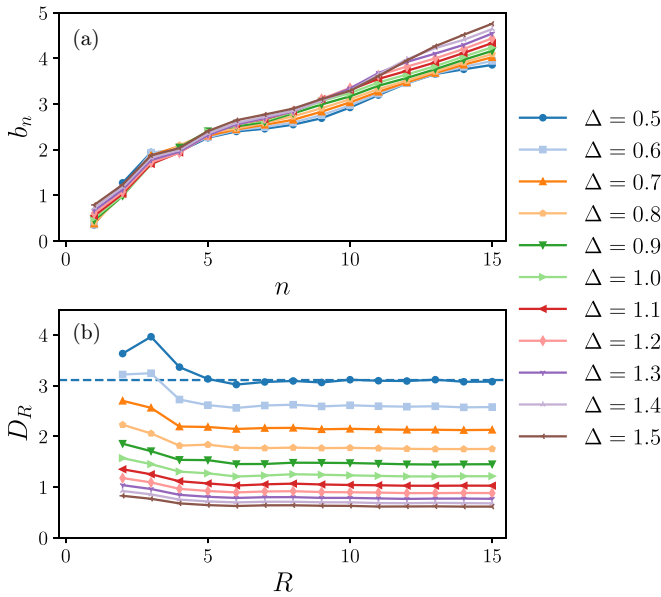
FIG. 1. Magnetization transport in the XXZ spin-1/2 chain with perturbation $\Delta' = 0.5$. (a) Lanczos coefficient b_n vs. n for various Δ. (b) Corresponding diffusion constants D_R. The dashed line indicates $D = 3.1$ from Ref. [52] for $\Delta = 0.5$.

vary visibly, thus indicating that an accurate result for the diffusion constants might have not yet been reached. This is different from the cases of the XXZ model and the XX ladder, where the D_R as obtained from Eq. (22) converge very quickly to the corresponding results from the literature.

Moreover, in the Appendixes, we compare our results in Figs. 1(b), 2(b), and 3(b) to the exact calculation of D in finite systems, based on the relation in Eq. (6). For the treatable
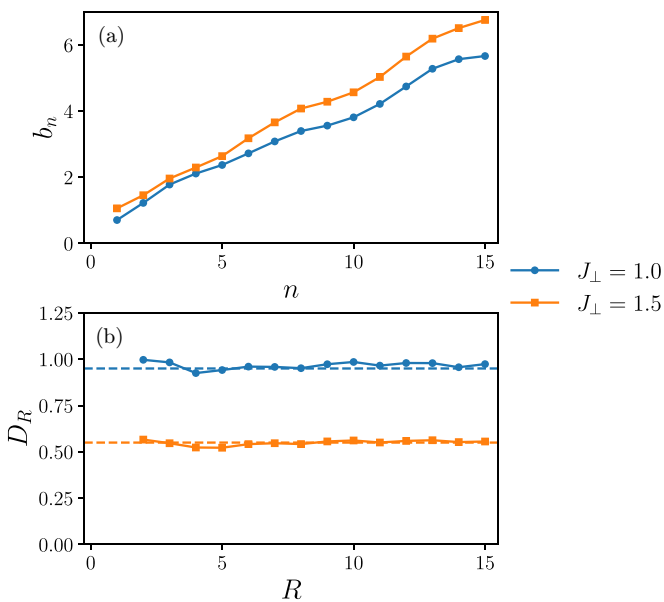

FIG. 2. Magnetization transport in the XX spin-1/2 ladder ($J_\parallel = 1$). (a) Lanczos coefficient b_n vs n for $J_\perp = 1.0, 1.5$. (b) Corresponding diffusion constants D_R. The dashed lines indicate $D = 0.95$ (from Refs. [47–49]) and $D = 0.55$ (from Ref. [47]) for $J_\perp = 1.0$ and $J_\perp = 1.5$, respectively.
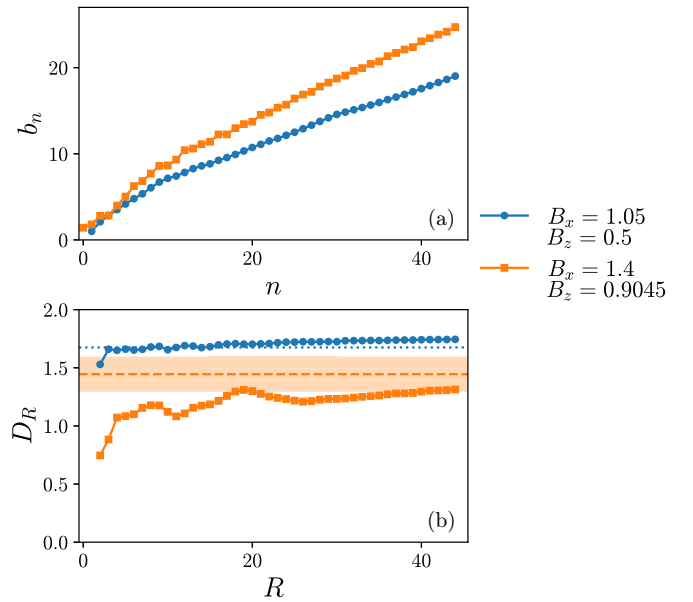

FIG. 3. Energy transport in the spin-1/2 Ising chain with a mixed field ($J = 1$). (a) Lanczos coefficient b_n vs n for various B_z. (b) Corresponding diffusion constants D_R. The dotted line indicates $D = 1.675$ [55] from Ref. [41] for $B_x = 1.05$, $B_z = 0.5$. The dashed line indicates $D = 1.44$ from Ref. [50] for $B_x = 1.4$, $B_z = 0.9045$ (see also Refs. [49,51]), and our result lies within a region of 10% (shaded area).

system sizes, we find convincing agreement, which supports the accuracy of the estimate.

V. CONCLUSION

In summary, we have discussed in this paper an alternative method for the accurate estimation of diffusion constants in quantum many-body systems, which is based on the recursion method. By employing the *operator growth hypothesis* in chaotic models, we have derived an estimate of the diffusion constant. For several examples, we have found convincing agreement of this estimate with results from the exact calculation in finite systems, and with existing results in the literature. In particular, we have observed that in many cases several of the first Lanczos coefficients are already sufficient to get a good estimate, which can be obtained resource-efficiently in comparison to other methods.

ACKNOWLEDGMENTS

APPENDIX A: DERIVATION OF EQ. (9)

In this section, we show the derivation of Eq. (9) in the main text. To this end, we define some $\mathcal{L}_n$ which is made from

$\mathcal{L}$ by erasing the first n row and the first n column:

$$\mathcal{L}_n = \sum_{m=n+1} b_m(|m+1)(m| + |m)(m+1|). \quad (A1)$$

$\mathcal{L}_n$ are Hermitian and we denote their eigenvectors by $|k_n)$:

$$\mathcal{L}_n|k_n) = E_{k_n}|k_n). \quad (A2)$$

Firstly, we focus on $\mathcal{L}_1$. Making use of the basis $\{|k_1), |0)\}$, $\mathcal{L}$ can be written as

$$\mathcal{L} = \sum_{k_1} b_1\{|k_1)(k_1|1)(0| + |0)(1|k_1)(k_1|\} + E_{k_1}|k_1)(k_1|. \quad (A3)$$

Now we switch to the interaction picture and taking $\mathcal{L}_1$ for the noninteracting system, the perturbation reads

$$\mathcal{V}_I(t) = \sum_{k_1} b_1\{|k_1)e^{-iE_{k_1}t}(k_1|1)(0| + |0)(1|k_1)e^{iE_{k_1}t}(k_1|\}. \quad (A4)$$

The time evolution in the interaction picture given by

$$i\frac{\partial}{\partial t}|\psi_I(t)) = \mathcal{V}_I(t)|\psi_I(t)), \quad (A5)$$

which in the basis $\{|k_1), |0)\}$ yields

$$\dot{r}_0 = -ib_1 \sum_{k_1}(1|k_1)e^{iE_{k_1}t}r_{k_1}$$
$$\dot{r}_{k_1} = -ib_1(k_1|1)e^{-iE_{k_1}t}r_0, \quad (A6)$$

where

$$r_0 = (0|\psi_I(t)), \quad r_{k_1} = (k_1|\psi_I(t)). \quad (A7)$$

Integrating the second equation of Eq. (A6), one obtains

$$r_{k_1}(t) = r_{k_1}(0) - ib_1(k_1|1) \int_0^t r_0(t')e^{-iE_{k_1}t'}dt'. \quad (A8)$$

Choosing $r_{k_1}(0) = 0$ and inserting Eq. (A8) into the first line of Eq. (A6) yields

$$\dot{r}_0(t) = -b_1^2 \int_0^t \sum_{k_1}|(k_1|1)|^2 e^{iE_{k_1}(t-t')}r_0(t')dt', \quad (A9)$$

which may be cast into the form of a standard integro-differential equations as

$$\dot{r}_0(t) = -\int_0^t K_1(t-t')r_0(t')dt', \quad (A10)$$

where

$$K_1(\tau) = \sum_{k_1} b_1^2|(k_1|1)|^2 e^{iE_{k_1}\tau}. \quad (A11)$$

The memory kernel $K_1(\tau)$ can also be written in a more compact form

$$K_1(\tau) = b_1^2 C_1(\tau), \quad (A12)$$

where

$$C_1(\tau) = (1|e^{i\mathcal{L}_1\tau}|1). \quad (A13)$$

Noting that the probability at $|0)$ are the same in the interaction picture as in the Schrödinger picture, one has

$$\dot{C}_0(t) = \dot{r}_0(t) = -b_1^2 \int_0^t C_1(t-t')C_0(t')dt'. \quad (A14)$$

Repeating the above procedure, it is easy to get

$$\dot{C}_n(t) = -b_{n+1}^2 \int_0^t C_{n+1}(t-t')C_n(t')dt', \quad (A15)$$

where $C_n(\tau)$ is defined as

$$C_n(\tau) = (n|e^{i\mathcal{L}_n\tau}|n). \quad (A16)$$

APPENDIX B: DERIVATIONS OF EQ. (19)

In this section, we show the detailed derivation of Eq. (19) in the main text. Inserting $b_n = \alpha n + \beta$ to Eq. (16) yields

$$\begin{aligned}
p_R &= \prod_{k=1}^{\infty} \frac{(b_{2k+R-1})^2}{b_{2k+R}b_{2k-2+R}} \\
&= \prod_{k=1}^{\infty} \frac{(\alpha(2k+R-1)+\beta)^2}{(\alpha(2k+R)+\beta)(\alpha(2k-2+R)+\beta)} \\
&= \prod_{k=1}^{\infty} \frac{\left(k + \frac{\alpha R+\beta}{2\alpha} - \frac{1}{2}\right)^2}{\left(k + \frac{\alpha R+\beta}{2\alpha}\right)\left(k + \frac{\alpha R+\beta}{2\alpha} - 1\right)}.
\end{aligned} \quad (B1)$$

Making use the following expression of Gamma function

$$\Gamma(z+1) = \prod_{k=1}^{\infty}\left[\frac{1}{1+\frac{z}{k}}\left(1+\frac{1}{k}\right)^z\right], \quad (B2)$$

it is easy to get

$$\frac{\Gamma(z-a+1)\Gamma(z+a+1)}{\Gamma^2(z+1)} = \prod_{k=1}^{\infty}\frac{(k+z)^2}{(k+z-a)(k+z+a)}. \quad (B3)$$

Comparing Eq. (B3) with Eq. (B1), and setting $z = \frac{R}{2} + \frac{\beta}{2\alpha} - \frac{1}{2}$, $a = \frac{1}{2}$, one has

$$p_R = \frac{\Gamma\left(\frac{R}{2} + \frac{\beta}{2\alpha}\right)\Gamma\left(\frac{R}{2} + \frac{\beta}{2\alpha} + 1\right)}{\Gamma^2\left(\frac{R}{2} + \frac{\beta}{2\alpha} + \frac{1}{2}\right)}, \quad (B4)$$

which is the result of Eq. (19).

APPENDIX C: LOGARITHMIC CORRECTION OF b_n

The derivation of our main result in Eq. (19) is based on a linear asymptotic form of Lanczos coefficient b_n. But it is shown in Ref. [41] that on top of the main linear behavior, for 1d system, there is a logarithmic correction for large n. In this section, we show that in this case, Eq. (19) still holds approximately.
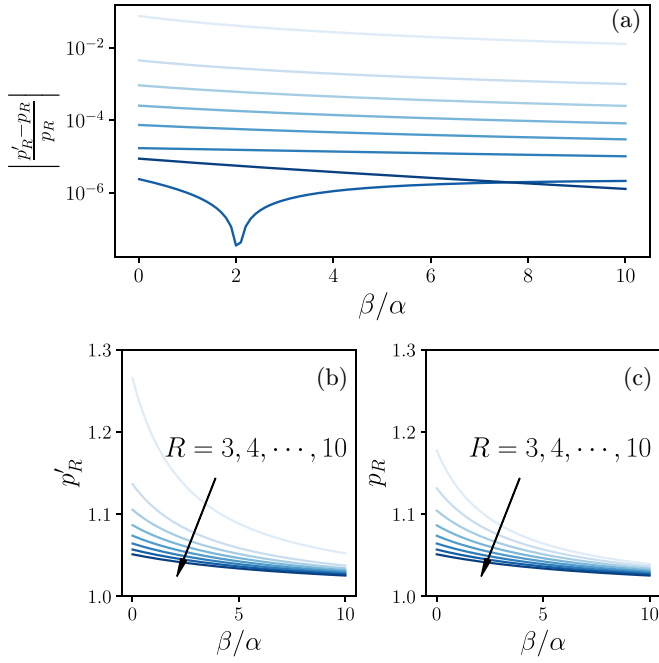
FIG. 4. (a) $|\frac{p'_R - p_R}{p_R}|$, (b) p'_R and (c) p_R vs β/α for various $R = 3, 4, \ldots, 10$ (from light to dark).

We consider p_R and p'_R which are defined as

$$p_R = \prod_{k=1}^{\infty} \frac{(b_{2k+R-1})^2}{b_{2k+R} b_{2k-1+R}}, \quad p'_R = \prod_{k=1}^{\infty} \frac{(b'_{2k+R-1})^2}{b'_{2k+R} b'_{2k-1+R}}, \quad (C1)$$

where

$$\begin{cases} b_n = \alpha n + \beta \\ b'_n = A\frac{n}{\ln n} + B \end{cases} \quad \text{for} \quad n \geqslant R. \quad (C2)$$

Here

$$A = \frac{(\ln R)^2}{\ln R - 1}\alpha, \quad B = \beta - \frac{\alpha R}{\ln R - 1}, \quad (C3)$$

are chosen such that the value of of b_n and b'_n as well as their first derivative coincide at $n = R$. Inserting Eq. (C2) to Eq. (C1), one gets

$$p'_R = \prod_{k=1}^{\infty} \frac{\left(\frac{2k+R-1}{\ln(2k+R-1)} + \frac{B}{A}\right)^2}{\left(\frac{2k+R}{\ln(2k+R)} + \frac{B}{A}\right)\left(\frac{2k+R-2}{\ln(2k+R-2)} + \frac{B}{A}\right)}, \quad (C4)$$

$$p_R = \prod_{k=1}^{\infty} \frac{\left(2k + R - 1 + \frac{\beta}{\alpha}\right)^2}{\left(2k + R + \frac{\beta}{\alpha}\right)\left(2k + R - 2 + \frac{\beta}{\alpha}\right)}. \quad (C5)$$

According to Eq. (C3) one has

$$\frac{B}{A} = \frac{\beta}{\alpha}\frac{\ln R - 1}{(\ln R)^2} - \frac{R}{(\ln R)^2}. \quad (C6)$$

From Eqs. (C4)–(C6), one can see that p'_R and p_R depend only on R and β/α. Different from p_R, we do not have an analytical expression for p'_R. But the convergence of the infinite product series in p'_R can be proved by making use of Leibniz criterion. In numerical simulations, p'_R is estimated by keeping the product series to $k = 5 \times 10^6$. In Fig. 4(a), we plot the difference between p'_R and p_R as a function of $\frac{\beta}{\alpha}$ for
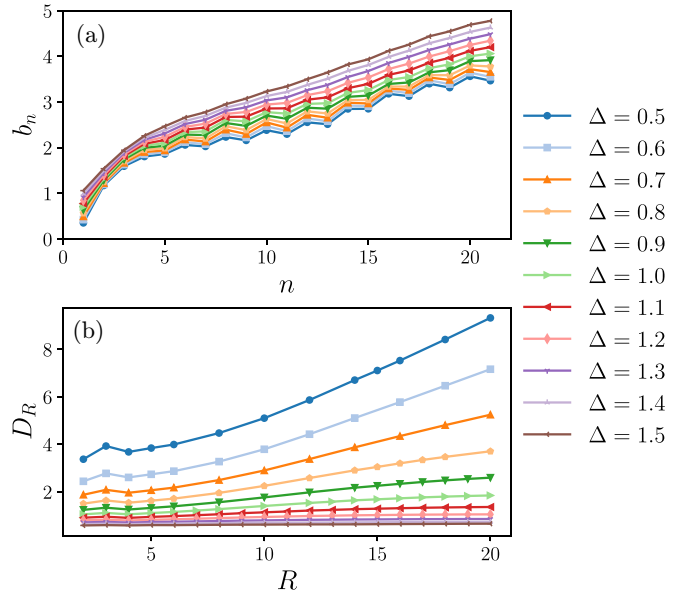

FIG. 5. Magnetization transport in the integrable XXZ spin-1/2 chain [defined in Eq. (D1)]. (a) Lanczos coefficient b_n vs n for various Δ. (b) Corresponding diffusion constants D_R.

various R. It is observed that for $R \geqslant 4$, the relative difference $|\frac{p'_R - p_R}{p_R}|$ is below 1% for all values of β/α we consider. It indicates that Eq. (19) still holds approximately in presence of the logarithmic correction. In addition, in Figs. 4(b) and 4(c), we show p'_R and p_R, from which one can see that both p'_R and p_R goes to 1 if either R or β/α goes to infinity.

APPENDIX D: DIFFUSION CONSTANT IN INTEGRABLE MODELS

In addition to the nonintegrable models studied in the main text, we also consider an integrable model, i.e., a spin-1/2 XXZ chain with only nearest-neighbor coupling,

$$H = \sum_{r=1}^{L} \left(s_r^x s_{r+1}^x + s_r^y s_{r+1}^y + \Delta s_r^z s_{r+1}^z\right). \quad (D1)$$

It is well-known that magnetization transport depends on the value of Δ [7]: it is ballistic at $\Delta < 1$, normal diffusive at $\Delta > 1$, and superdiffusive at $\Delta = 1$. In Fig. 5, we show the estimation of the diffusion constant by Eq. (22) in the main text. A substantial difference in the behavior of D_R is observed for $\Delta < 1$ compared to $\Delta > 1$: D_R appears to diverge for $\Delta < 1$ and tends to converge to some finite value for $\Delta > 1$. The (seemingly) divergence of D_R is due to the pronounced even-odd effect, in addition to the dominant linear increase of Lanczos coefficients, i.e.,

$$b_n \sim \alpha n + \beta + (-1)^n \gamma_n. \quad (D2)$$

Here, we are not aiming at a precise location of the transition from ballistic to diffusive transport by making use of the recursion method. This would definitely need the knowledge of infinite number of Lanczos coefficient, which is clearly beyond the reach of the numerical method at hand. The primary objective of this example is to show that "finite size scaling"
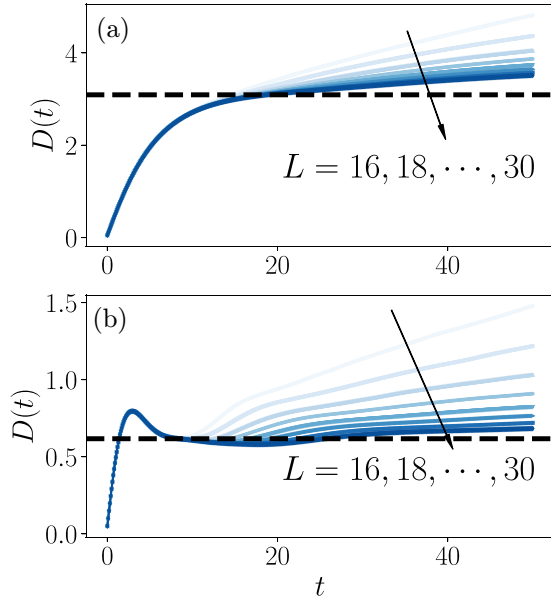
FIG. 6. Time-dependent diffusion constant $D(t)$ in the XXZ chain with parameters $\Delta' = 0.5$ and (a) $\Delta = 0.5$ and (b) $\Delta = 1.5$, for system size $L = 16, 18, \ldots, 30$ (from light to dark). The dashed line indicates the average value of the last five D_R shown in Fig. 1 (b). For (a), data for larger system sizes $L = 33$ can also be found in Ref. [52].

of D_R (dependence of D_R on R) can at least show some hint on the onset of the ballistic (or at least superdiffusive) behavior, particularly when an overall increase of D_R is observed.

APPENDIX E: TIME-DEPENDENT DIFFUSION CONSTANT IN FINITE-SIZE SYSTEMS

In the spin-1/2 XXZ chain and XX ladder, we consider the spin current

$$J_S = \begin{cases} \sum_{r=1}^{L} \left(s_r^x s_{r+1}^y - s_r^y s_{r+1}^x \right), & \text{XXZ} \\ J_\parallel \sum_{r=1}^{L/2} \sum_{k=1}^{2} \left(s_{r,k}^x s_{r+1,k}^y - s_{r,k}^y s_{r+1,k}^x \right), & \text{XX} \end{cases} \quad (E1)$$

with the time-dependent diffusion coefficient

$$D(t) = \frac{1}{\chi} \int_0^t \langle J_S(t') J_S \rangle \, dt', \quad \chi = \frac{L}{4}. \quad (E2)$$

In the mixed-field Ising model, we instead consider the energy-current operator

$$J_E = 4B_x \sum_{r=1}^{L} s_r^y \left(s_{r+1}^z - s_{r-1}^z \right) \quad (E3)$$

with the time-dependent diffusion constant

$$D(t) = \frac{1}{\chi} \int_0^t \langle J_E(t') J_E \rangle \, dt', \quad \chi = L(B_x^2 + B_z^2 + 1). \quad (E4)$$

In Figs. 6–8, we calculate the time-dependent diffusion coefficient $D(t)$ for finite systems, using dynamical typicality [26,27]. In all three models, we can see a tendency that the long-time value $D(t)$ becomes closer to our estimation $\overline{D_R}$
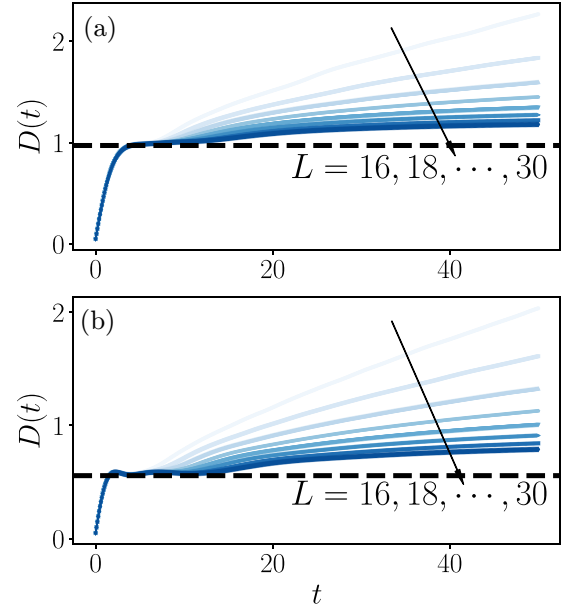

FIG. 7. Time-dependent diffusion constant $D(t)$ in the XX ladder with parameters $J_\parallel = 1.0$ and (a) $J_\perp = 1.0$; (b) $J_\perp = 1.5$, for system size $L = 16, 18, \ldots, 30$ (from light to dark). The dashed line indicates the average value of the last five D_R shown in Fig. 2(b). Data for larger system sizes $L = 34$ can also be found in Ref. [47].

(average over the last 5 values) for larger L. Whether or not this value will converge to $\overline{D_R}$ is in principle not clear, due to the limited system size ($L \leqslant 30$). But based on the results, it is reasonable to expect that the diffusion constant $D(L \to \infty)$ is close to $\overline{D_R}$.
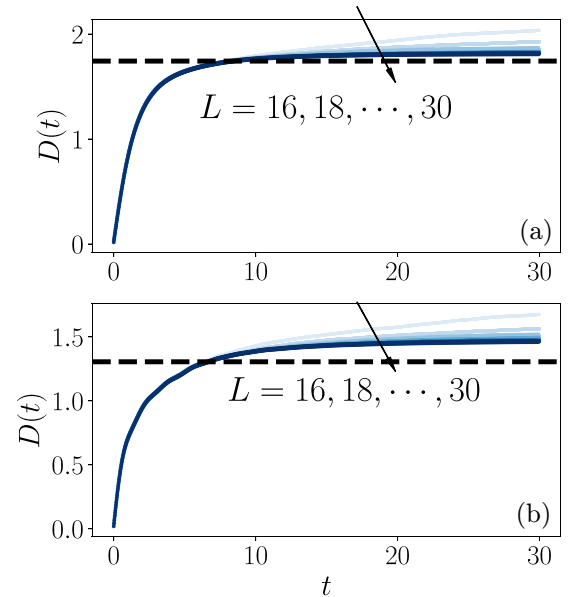

FIG. 8. Time-dependent diffusion constant $D(t)$ in the mixed-field Ising chain with parameters (a) $B_z = 0.5$, $B_x = 1.05$ and (b) $B_z = 0.9045$, $B_x = 1.4$, for system size $L = 16, 18, \ldots, 30$ (from light to dark). The dashed line indicates the average value of the last five D_R shown in Fig. 3(b). Data for larger system sizes can also be found in Refs. [49–51].

[1] I. Bloch, J. Dalibard, and W. Zwerger, Many-body physics with ultracold gases, Rev. Mod. Phys. **80**, 885 (2008).

[2] A. Polkovnikov, K. Sengupta, A. Silva, and M. Vengalattore, *Colloquium*: Nonequilibrium dynamics of closed interacting quantum systems, Rev. Mod. Phys. **83**, 863 (2011).

[3] T. Langen, R. Geiger, and J. Schmiedmayer, Ultracold atoms out of equilibrium, Annu. Rev. Condens. Matter Phys. **6**, 201 (2015).

[4] J. Eisert, M. Friesdorf, and C. Gogolin, Quantum many-body systems out of equilibrium, Nat. Phys. **11**, 124 (2015).

[5] L. D'Alessio, A. Polkovnikov, Y. Kafri and M. Rigol, From quantum chaos and eigenstate thermalization to statistical mechanics and thermodynamics, Adv. Phys. **65**, 239 (2016).

[6] D. A. Abanin, E. Altman, I. Bloch, and M. Serbyn, *Colloquium*: Many-body localization, thermalization, and entanglement, Rev. Mod. Phys. **91**, 021001 (2019).

[7] B. Bertini, F. Heidrich-Meisner, C. Karrasch, T. Prosen, R. Steinigeweg, and M. Žnidarič, Finite-temperature transport in one-dimensional quantum lattice models, Rev. Mod. Phys. **93**, 025003 (2021).

[8] J.-S. Caux and J. Mossel, Remarks on the notion of quantum integrability, J. Stat. Mech. (2011) P02023.

[9] X. Zotos, F. Naef, and P. Prelovšek, Transport and conservation laws, Phys. Rev. B **55**, 11029 (1997).

[10] T. Prosen, Open *XXZ* spin chain: Nonequilibrium steady state and a strict bound on ballistic transport, Phys. Rev. Lett. **106**, 217206 (2011).

[11] T. Prosen and E. Ilievski, Families of quasilocal conservation laws and quantum spin transport, Phys. Rev. Lett. **111**, 057203 (2013).

[12] A. Bastianello, B. Bertini, B. Doyon, and R. Vasseur, Introduction to the special issue on emergent hydrodynamics in integrable many-body systems, J. Stat. Mech. (2022) 014001.

[13] B. Doyon, S. Gopalakrishnan, F. Møller, J. Schmiedmayer, and R. Vasseur, Generalized hydrodynamics: A perspective, arXiv:2311.03438.

[14] R. Nandkishore and D. A. Huse, Many-body localization and thermalization in quantum statistical mechanics, Annu. Rev. Condens. Matter Phys. **6**, 15 (2015).

[15] D. J. Luitz and Y. B. Lev, The ergodic side of the many-body localization transition, Ann. Phys. **529**, 1600350 (2017).

[16] K. R. A. Hazzard, M. van den Worm, M. Foss-Feig, S. R. Manmana, E. G. Dalla Torre, T. Pfau, M. Kastner, and A. M. Rey, Quantum correlations and entanglement in far-from-equilibrium spin systems, Phys. Rev. A **90**, 063622 (2014).

[17] B. Kloss and Y. B. Lev, Spin transport in a long-range-interacting spin chain, Phys. Rev. A **99**, 032114 (2019).

[18] A. G. Burchards, J. Feldmeier, A. Schuckert, and M. Knap, Coupled hydrodynamics in dipole-conserving quantum systems, Phys. Rev. B **105**, 205127 (2022).

[19] A. Morningstar, N. O'Dea, and J. Richter, Hydrodynamics in long-range interacting systems with center-of-mass conservation, Phys. Rev. B **108**, L020304 (2023).

[20] P. Jung, R. W. Helmes, and A. Rosch, Transport in almost integrable models: Perturbed Heisenberg chains, Phys. Rev. Lett. **96**, 067202 (2006).

[21] P. Jung and A. Rosch, Spin conductivity in almost integrable spin chains, Phys. Rev. B **76**, 245108 (2007).

[22] R. Steinigeweg, J. Herbrych, X. Zotos, and W. Brenig, Heat conductivity of the Heisenberg spin-1/2 ladder: From weak to strong breaking of integrability, Phys. Rev. Lett. **116**, 017202 (2016).

[23] F. Heidrich-Meisner, A. Honecker, and W. Brenig, Transport in quasi one-dimensional spin-1/2 systems, Eur. Phys. J.: Spec. Top. **151**, 135 (2007).

[24] M. W. Long, P. Prelovšek, S. El Shawish, J. Karadamoglou, and X. Zotos, Finite-temperature dynamical correlations using the microcanonical ensemble and the Lanczos algorithm, Phys. Rev. B **68**, 235106 (2003).

[25] P. Prelovšek, S. E. Shawish, X. Zotos, and M. Long, Anomalous scaling of conductivity in integrable fermion systems, Phys. Rev. B **70**, 205129 (2004).

[26] F. Jin, D. Willsch, M. Willsch, H. Lagemann, K. Michielsen, and H. De Raedt, Random state technology, J. Phys. Soc. Jpn. **90**, 012001 (2021).

[27] T. Heitmann, J. Richter, D. Schubert, and R. Steinigeweg, Selected applications of typicality to real-time dynamics of quantum many-body systems, Z. Naturforsch. A **75**, 421 (2020).

[28] S. Langer, F. Heidrich-Meisner, J. Gemmer, I. P. McCulloch, and U. Schollwöck, Real-time study of diffusive and ballistic transport in spin-$\frac{1}{2}$ chains using the adaptive time-dependent density matrix renormalization group method, Phys. Rev. B **79**, 214409 (2009).

[29] C. Karrasch, J. H. Bardarson, and J. E. Moore, Finite-temperature dynamical density matrix renormalization group and the Drude weight of spin-1/2 chains, Phys. Rev. Lett. **108**, 227206 (2012).

[30] C. Karrasch, J. E. Moore, and F. Heidrich-Meisner, Real-time and real-space spin and energy dynamics in one-dimensional spin-$\frac{1}{2}$ systems induced by local quantum quenches at finite temperatures, Phys. Rev. B **89**, 075139 (2014).

[31] J. V. Alvarez and C. Gros, Low-temperature transport in Heisenberg chains, Phys. Rev. Lett. **88**, 077203 (2002).

[32] S. Grossjohann and W. Brenig, Hydrodynamic limit for the spin dynamics of the Heisenberg chain from quantum Monte Carlo calculations, Phys. Rev. B **81**, 012404 (2010).

[33] T. Prosen and M. Žnidarič, Matrix product simulations of nonequilibrium steady states of quantum spin chains, J. Stat. Mech. (2009) P02035.

[34] M. Žnidarič, Spin transport in a one-dimensional anisotropic Heisenberg model, Phys. Rev. Lett. **106**, 220601 (2011).

[35] H. Wichterich, M. J. Henrich, H.-P. Breuer, J. Gemmer, and M. Michel, Modeling heat transport through completely positive maps, Phys. Rev. E **76**, 031115 (2007).

[36] J. Wurtz and A. Polkovnikov, Quantum diffusion in spin chains with phase space methods, Phys. Rev. E **101**, 052120 (2020).

[37] D. Schubert, J. Richter, F. Jin, K. Michielsen, H. De Raedt, and R. Steinigeweg, Quantum versus classical dynamics in spin models: Chains, ladders, and square lattices, Phys. Rev. B **104**, 054415 (2021).

[38] A. J. McRoberts, T. Bilitewski, M. Haque, and R. Moessner, Anomalous dynamics and equilibration in the classical Heisenberg chain, Phys. Rev. B **105**, L100403 (2022).

[39] V. S. Viswanath and G. Müller, *The Recursion Method: Application to Many Body Dynamics* (Springer, Berlin, 1994).

[40] C. Joslin and C. Gray, Calculation of transport coefficients using a modified Mori formalism, Mol. Phys. **58**, 789 (1986).

[41] D. E. Parker, X. Cao, A. Avdoshkin, T. Scaffidi, and E. Altman, A universal operator growth hypothesis, Phys. Rev. X **9**, 041017 (2019).

[42] A. Dymarsky and A. Gorsky, Quantum chaos as delocalization in Krylov space, Phys. Rev. B **102**, 085137 (2020).

[43] S. Bhattacharyya, A. De, S. Gazit, and A. Auerbach, Metallic transport of hard-core bosons, Phys. Rev. B **109**, 035117 (2024).

[44] Z.-X. Cai, S. Sen, and S. D. Mahanti, Long-time dynamics via direct summation of infinite continued fractions, Phys. Rev. Lett. **68**, 1637 (1992).

[45] S. Sen, Z.-X. Cai, and S. D. Mahanti, Dynamical correlations and the direct summation method of evaluating infinite continued fractions, Phys. Rev. E **47**, 273 (1993).

[46] M. H. Lee, Ergodic theory, infinite products, and long time behavior in Hermitian models, Phys. Rev. Lett. **87**, 250601 (2001).

[47] R. Steinigeweg, F. Heidrich-Meisner, J. Gemmer, K. Michielsen, and H. De Raedt, Scaling of diffusion constants in the spin-$\frac{1}{2}$ XX ladder, Phys. Rev. B **90**, 094417 (2014).

[48] B. Kloss, Y. B. Lev, and D. Reichman, Time-dependent variational principle in matrix-product state manifolds: Pitfalls and potential, Phys. Rev. B **97**, 024307 (2018).

[49] T. Rakovszky, C. W. von Keyserlingk, and F. Pollmann, Dissipation-assisted operator evolution method for capturing hydrodynamic transport, Phys. Rev. B **105**, 075131 (2022).

[50] S. N. Thomas, B. Ware, J. D. Sau, and C. D. White, Comparing numerical methods for hydrodynamics in a 1D lattice model, arXiv:2310.06886.

[51] C. Artiaco, C. Fleckenstein, D. Aceituno, T. K. Kvorning, and J. H. Bardarson, Efficient large-scale many-body quantum dynamics via local-information time evolution, PRX Quantum **5**, 020352 (2024).

[52] J. Richter and R. Steinigeweg, Combining dynamical quantum typicality and numerical linked cluster expansions, Phys. Rev. B **99**, 094419 (2019).

[53] R. Steinigeweg and J. Gemmer, Density dynamics in translationally invariant spin-$\frac{1}{2}$ chains at high temperatures: A current-autocorrelation approach to finite time and length scales, Phys. Rev. B **80**, 184402 (2009).

[54] H. Mori, Transport, collective motion, and Brownian motion, Prog. Theor. Phys. **33**, 423 (1965).

[55] Due to differences in the definition, the value of the diffusion constant reported in Fig. 7 of Ref. [41] differs from that in our paper by a factor of 2. More specifically, $D = 3.35$ in Ref. [41] corresponds to $D = 1.675$ in ours. The parameters $J = 1$, $B_x = 1.05$, $B_z = 0.5$ considered here is equivalent to the parameters considered in Fig. 7 of Ref. [41].